RECORD
2024/1

INTRODUCTION TO GEOCHRONOLOGY INFORMATION, 2024

IOH Fielding, RE Turnbull and Y Lu

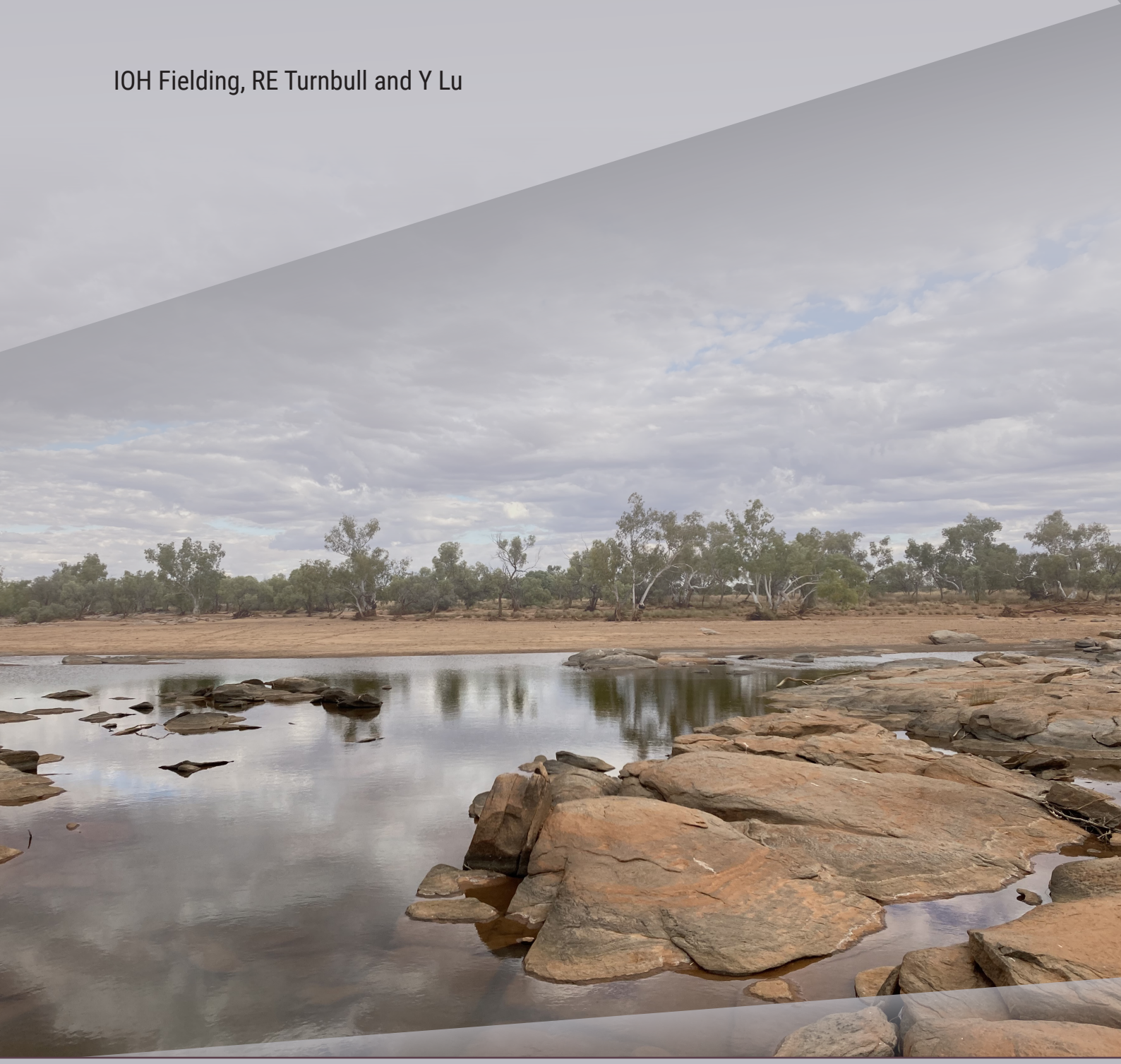

GOVERNMENT OF WESTERN AUSTRALIA
Department of **Energy, Mines, Industry Regulation and Safety**
Geological Survey of Western Australia

Government of **Western Australia**
Department of **Mines, Industry Regulation and Safety**

RECORD 2024/1

INTRODUCTION TO GEOCHRONOLOGY INFORMATION, 2024

IOH Fielding, RE Turnbull and Y Lu

PERTH 2024

Geological Survey of Western Australia

REFERENCE
The recommended reference for this publication is:
Fielding, IOH, Turnbull, RE and Lu, Y 2024, Introduction to geochronology information, 2024: Geological Survey of Western Australia, Record 2024/1, 8p.

ISBN 978-1-74168-035-5
ISSN 2204-4345

About this publication
Zircon and monazite analyses were conducted in part using the SHRIMP ion microprobes in the John de Laeter Centre (JdLC) at Curtin University, operated with financial support of the Australian Research Council and AuScope National Collaborative Research Infrastructure Strategy (NCRIS). LA-ICP-MS instruments in the GeoHistory Facility of the JdLC at Curtin University were funded via an Australian Geophysical Observing System grant provided to AuScope Limited by the AQ44 Australian Education Investment Fund program or via funding from the Australian Research Council LIEF program (LE150100013). Analyses were also conducted using the facilities and scientific and technical assistance of Microscopy Australia at the Centre for Microscopy, Characterization and Analysis (CMCA), at The University of Western Australia (UWA), a facility funded by the University, State and Commonwealth Governments. LA-ICP-MS instruments in the CMCA were funded by the Australian Research Council (LE150100013). Allen Kennedy, Noreen Evans, Hao Gao, and Brad McDonald, all of Curtin University, as well as Chris Fisher and Tony Kemp at UWA, are thanked for technical assistance.

The TESCAN Integrated Mineral Analyser (TIMA) instrument was funded by a grant from the Australian Research Council (LE140100150) and is operated by the JdLC with the support of the Geological Survey of Western Australia (GSWA), UWA and Murdoch University.

Disclaimer

Acknowledgement of Country
We respectfully acknowledge Aboriginal peoples as the Traditional Custodians of this land on which we deliver our services to the communities throughout Western Australia. We acknowledge their enduring connection to the lands, waterways and communities and pay our respects to Elders past and present.

Published 2024 by the Geological Survey of Western Australia
This Record is published in digital format (PDF) and is available online at <www.dmirs.wa.gov.au/GSWApublications>.

Further details of geoscience products are available from:
First Floor Counter
Department of Energy, Mines, Industry Regulation and Safety
100 Plain Street
EAST PERTH WESTERN AUSTRALIA 6004
Telephone: +61 8 9222 3459 Email: publications@dmirs.wa.gov.au
www.dmirs.wa.gov.au/GSWApublications

Cover image: One of the largest and most distinctive metagranitic units in the Gascoyne Province, the c. 1670 to 1648 Ma Davey Well Granite emerges from the water of the Yinnetharra Pool along the Gascoyne River. Photo by Angela Riganti

Contents

Tables

Introduction to Geochronology Information, 2024

IOH Fielding, RE Turnbull and Y Lu

Abstract

Geochronology is a fundamental component of the geoscience studies at the Geological Survey of Western Australia (GSWA). The geochronology program determines precise and accurate ages of minerals, rocks and geological events to understand the geological history of Western Australia and contributes to enhancing the prospectivity of the State. Here we document the background analytical details of a range of geochronological techniques, including the Sensitive High Resolution Ion Microprobe (SHRIMP) and laser ablation inductively coupled plasma mass spectrometry (LA-ICP-MS), which have been applied at GSWA to constrain the timing of magmatism, metamorphism, deformation, hydrothermal activity and mineralization.

KEYWORDS: geochronology, LA-ICP-MS, SHRIMP

Introduction

This introduction provides background analytical details for Geochronology Records released by the Geological Survey of Western Australia (GSWA) during 2024. Most results are U–Th–Pb age determinations obtained by sensitive high resolution ion microprobe (SHRIMP) or laser ablation inductively coupled plasma mass spectrometry (LA-ICP-MS). Analytical details for samples dated using other methods and decay schemes (e.g. Rb–Sr, Lu–Hf, K–Ar, $^{40}Ar/^{39}Ar$, Re–Os) are provided within the individual Geochronology Records for those samples. Each Geochronology Record describes the sample analysed and analytical results obtained and provides a brief interpretation of the results. The broader geological implications of the data may be published elsewhere. Some Records describe results for samples analysed by collaborators external to GSWA, in which case additional analytical information not detailed in this document may be included within the individual Records. Release of new Geochronology Records to the web <www.demirs.wa.gov.au/geochron> occurs throughout the year as Records are completed.

Most samples have been assigned to tectonic or stratigraphic units based on the interpretation of geochronological results and field relationships at the time of publication. These assignments, and the currency of stratigraphic and tectonic units, may subsequently be revised and up-to-date information should be obtained from the latest GSWA publications. Sample location grid references in Geochronology Records refer to the Geocentric Datum of Australia 1994 (GDA94). Locality coordinates most samples were obtained using a hand-held Global Positioning System (GPS) receiver, are accurate to better than ±100 m, and are referenced using Map Grid Australia (MGA) coordinates.

Analytical techniques

SHRIMP U–Pb geochronology of zircon and baddeleyite accounts for the majority of isotope measurements made by GSWA. The high spatial resolution (5–30 µm) of the SHRIMP enables measurements of growth zones of different ages within complex crystals, and permits damaged areas of crystals to be avoided. Each analysis takes 12–15 minutes, and about 40–50 analyses can typically be obtained during a 24-hour session. SHRIMP geochronology is conducted in real time, and analytical protocols are optimized for each sample as its isotopic characteristics become apparent.

LA-ICP-MS U–Pb geochronology is a versatile and more rapid technique that enables several hundred analyses to be obtained in a 24-hour session. The volume sampled by the laser during zircon analysis is typically 30–50 µm diameter by 30 µm deep, hence the analysis can include material that is damaged or contains unobserved cracks or inclusions. The method is therefore ideal for detrital zircon and other samples in which statistically large datasets are required, and where the crystals are relatively large and in good condition (i.e. not damaged by radiation and with few cracks or inclusions). Samples containing damaged or complex crystals are typically analysed by GSWA using the SHRIMP, which has a much smaller sampling volume, typically 15–25 µm diameter for zircon, and 1–2 µm deep, and can more easily target areas most favourable for analysis. Similar considerations are applicable to LA-ICP-MS U–Pb geochronology of monazite, although the typical laser diameter for monazite (e.g. 7–20 µm) means the sampling volume is relatively small and problematic areas of crystals can often be avoided.

The quadrupole LA-ICP-MS is also used to measure trace element compositions of previously dated separated zircons (e.g. Lu et al., 2016, 2019). In this case, zircon compositions are of primary interest and the precision of U–Pb data may be lower, depending on the number of trace elements chosen for concurrent analysis, as a long element list diminishes the fraction of the ion signal available for U–Pb measurements.

Laser ablation split stream (LASS) techniques are used for in situ analysis of monazite and other minerals in thin section, and involve splitting the ablated products between a multi-collector ICP-MS (MC-ICP-MS) for U–Th–Pb geochronology and a quadrupole ICP-MS for trace elements.

GSWA uses the SHRIMP and LA-ICP-MS instruments, the Tescan Integrated Mineral Analyser (TIMA) and other scanning electron microscopes, in the John de Laeter Centre at Curtin University and in the Centre for Microscopy, Characterisation and Analysis (CMCA) at The University of Western Australia (UWA). GSWA's analytical program is supported by world-class sample preparation services provided in-house by the GSWA laboratory at the Perth Core Library.

SHRIMP analytical procedures

Sample preparation

Rock samples are trimmed of weathered surfaces and secondary veins using a rock saw. The cleaned material is washed, and then crushed to centimetre-size fragments using a customized mechanical jaw-crusher that is disassembled and cleaned prior to the processing of each sample. Between 0.5 and 4 kg of the resulting rock fragments are ground in a low-chromium steel ring-mill, using the minimum grinding time necessary for the resulting powder to pass through a disposable nylon sieve cloth with a mesh size of 400 µm. Very fine particles are removed and discarded from the sieved powder by elutriation, in batches of about 300 g, using filtered water under controlled flow conditions (400–2400 mL·min^{-1}), and a 2000 ml glass funnel apparatus designed and constructed by GSWA's laboratory. The remaining fraction is dried overnight in an oven at 90 °C, before being split into batches of <150 g. Each batch is then mixed with sodium polytungstate solution ($Na_6[H_2W_{12}O_{40}]\cdot H_2O$), which has a density of about 2.9 g·cm^{-3} at 20 °C, in 1000 ml glass separating funnels. The funnels are periodically agitated to facilitate density separation.

The heavy mineral concentrate is drained from each funnel onto a filter paper, washed thoroughly with distilled water and acetone in a Büchner vacuum funnel, and oven-dried overnight at 90°C. Highly magnetic minerals are removed using a hand magnet, followed by one or more passes through a rotating rare earth element (REE) magnetic separator, also designed at the GSWA laboratory. The remaining material is processed using a Frantz isodynamic magnetic separator. For the first pass, a longitudinal tilt of 20°, a transverse tilt of 10°, and a magnet current of 0.2 – 0.8 A are employed. The non-magnetic fraction from the first pass is reprocessed using higher tilt settings and current values that vary on an individual sample basis. All fractions from each sample are retained in storage.

The resulting non-magnetic fraction is treated with methylene iodide (CH_2I_2), using a sensitive, miniaturized 'double-tube' method (Bastian, 1994). This involves using a 16 mm diameter test tube into which a 1.5 mm diameter constriction has been placed, so that an open, bell-shaped chamber is present at its base. The constriction is small enough that the heavy liquid is held in the upper chamber by its meniscus when the top of the tube is stoppered. The constricted tube is placed into a larger test tube containing methylene iodide, which has a density of about 3.3 g·cm^{-3} at 20 °C. The heavy mineral concentrate is carefully poured into the inner tube, the contents are gently stirred, and the inner tube is gently rotated and tilted. Minerals with densities greater than 3.3 g·cm^{-3} fall past the constriction to settle in the outer test tube. When separation is complete, the inner tube is stoppered, slowly lifted out, and the contents washed with acetone onto a filter paper. The purified heavy mineral concentrate in the outer test tube is collected on a second filter paper.

Zircon, monazite or baddeleyite crystals are then hand picked from the heavy mineral separate with the aid of a binocular microscope. In general, up to 150–200 representative crystals are selected for igneous and metamorphic rocks, and all or most grains are picked for sedimentary rocks containing detrital zircons. Crystals are mounted in 25 mm diameter epoxy disks, and the mount surface polished to expose the grain interiors. Each mount typically contains minerals from one, two or several different samples, which are aligned in rows, together with several crystals or crystal fragments of reference materials (details in Table 1).

Mineral imaging and target selection

Each mount is photographed in transmitted and reflected light, and in reflected light using a differential interference contrast (Nomarski) filter, at magnifications of 70–150x. The mount is then ultrasonically cleaned in ethanol, petroleum ether, and detergent solution (Decon), then rinsed in distilled and deionized water, and dried in an oven at 60 °C. The polished surface of the mount is then coated evaporatively with high-purity gold to a thickness of about 40 nm, to achieve an edge-to-edge resistance of 15–25 ohms.

To reveal the internal structures of zircons, cathodoluminescence (CL) imaging of all zircons on the mount is undertaken prior to analysis. For each sample, sufficient images are acquired to provide complete coverage of the mounted crystals. Backscattered-electron (BSE) images are employed for baddeleyite and monazite. Mineral crystals to be analysed are selected based on their combined CL (or BSE), reflected-light, and transmitted-light characteristics.

SHRIMP U–Pb analysis

Uranium, thorium and lead isotope measurements of zircon are based on procedures described by Compston et al. (1984) and Claoué-Long et al. (1995), with modifications summarized by Williams (1998). Procedures for baddeleyite follow Wingate et al. (1998). Procedures for monazite analysis follow Williams et al. (1996), with modifications by Kinny (1997). For zircon and baddeleyite analysis, a 15–30 µm diameter primary beam of O_2^- ions at 10 keV, purified by means of a Wien filter, is employed to sputter secondary ions from the surface of each target mineral. The net primary ion current, as measured leaving the sample, is typically between 1.0 and 2.5 nA. Secondary ions are accelerated to 10 keV, energy-filtered by passage through a cylindrical 85° electrostatic analyser with a turning radius of 1.27 m, and mass-filtered using a 72.5° magnet sector with a turning radius of 1 m. Secondary ions are counted

by switching the magnetic field to direct the secondary ion beam into an electron multiplier, used in pulse-counting mode. During the analytical session, the secondary ion analyser is set to a mass resolution of ≥5000 (1% peak-height definition), which is sufficient to resolve lead isotopes from most potential molecular interferences. The magnetic field is cycled to select isotopic masses in the following sequence (in atomic mass units [amu]): 196 (species $[^{90}Zr_2{}^{16}O]^+$, count time 2 s), 204 ($^{204}Pb^+$, 10 s), c. 204.1 (background, 10 s), 206 ($^{206}Pb^+$, 10 s), 207 ($^{207}Pb^+$, 20–40 s), 208 ($^{208}Pb^+$, 10 s), 238 ($^{238}U^+$, 5 s), 248 ($[^{232}Th^{16}O]^+$, 5 s), and 254 ($[^{238}U^{16}O]^+$, 2 s). Data are collected for six cycles through the mass stations for the dating of minerals from igneous or metamorphic rocks. This is reduced to five cycles for the dating of detrital zircons from sedimentary rocks to maximize the number of crystals that can be analysed during the session.

SHRIMP monazite analyses are similar to those of zircon, although a lower-intensity primary ion beam can be used, owing to higher secondary-ion count rates on the species of interest. Typically, a 7–15 µm diameter primary beam, with an intensity of about 0.5 nA, is employed. Ion microprobe analyses of monazite are affected by an uneven background spectrum of scattered ions (Kinny, 1997), which can be reduced effectively by use of the SHRIMP retardation lens system, which is set at about 10 kV. This discriminates against low-energy ions entering the collector. Each analysis consists of six cycles through the isotopic masses in the following sequence (in amu): 202 (species $[^{139}La^{31}P^{16}O_2]^+$, count time 2 s), 203 ($[^{140}Ce^{31}P^{16}O_2]^+$, 2 s), 204 ($^{204}Pb^+$, 10 s), ~204.1 (background, 10 s), 206 ($^{206}Pb^+$, 10 s), 207 ($^{207}Pb^+$, 30 s), 208 ($^{208}Pb^+$, 5 s), 232 ($^{232}Th^+$, 5 s), 254 ($[^{238}U^{16}O]^+$, 5 s), 264 ($[^{232}Th^{16}O_2]^+$, 2 s), and 270 ($[^{238}U^{16}O_2]^+$, 3 s).

Standards for SHRIMP U/Pb calibration in zircon and baddeleyite include CZ3, Temora 2, M257, BR266, and PBR2 (Table 1). To monitor the accuracy of $^{207}Pb/^{206}Pb$ ratios, crystals of OGC1 zircon or PBR2 baddeleyite are included on each mount. The CZ3, M257 or BR266 zircon standards are used for uranium concentration calibration. Several zircons with high ^{238}U and Pb contents are also added to each zircon or baddeleyite mount to facilitate setup of the mass peaks on the ion microprobe. For SHRIMP monazite analysis, the India monazite standard is used for U/Pb calibration, whereas the GM3 monazite standard is used to monitor the accuracy of $^{207}Pb/^{206}Pb$ ratios.

SHRIMP data reduction

SHRIMP U–Pb zircon, baddeleyite and monazite data are reduced using SQUID 2.50 and Isoplot 3.71 (add-ins for Microsoft Excel; Ludwig, 2003, 2009) with decay constants recommended by Steiger and Jäger (1977). Ratios of $^{206}Pb^+/^{238}U^+$ in zircon are calibrated to the known $^{206}Pb/^{238}U$ of the zircon standard (Table 1), using a power-law relationship between $^{206}Pb^+/^{238}U^+$ and UO^+/U^+, with a fixed exponent of 2.0 (determined empirically from measurements of zircon standards over several years; Claoué-Long et al., 1995). In most cases, data are corrected for the presence of common Pb using measured $^{204}Pb/^{206}Pb$ (Compston et al., 1984). An average crustal composition (Stacey and Kramers, 1975), appropriate to the age of the mineral, is assumed, although in most cases corrections are sufficiently small to be insensitive to the choice of common-Pb composition. Prior to analysis, each site is cleaned by rastering the primary ion beam over the area for two to three minutes. Subsequently, $^{204}Pb^+$ counts for most analyses remain low and constant, and show no tendency to decrease over the course of a 12–15-minute analysis, implying that common Pb is mainly inherent to the mineral, rather than a surface contaminant of the grain.

In a minority of cases, mainly in relatively young (Mesoproterozoic and younger), low-uranium zircons, 204-corrected $^{207}Pb^*/^{206}Pb^*$ (Pb* indicates radiogenic Pb) ratios are observed to correlate with their common-Pb corrections (i.e. the fraction (f204) of common ^{206}Pb in total ^{206}Pb), indicating that the corrections using ^{204}Pb are inaccurate for some or all analyses. In these cases, the 204-correction is abandoned in favour of a regression from initial Pb. This method assumes that the total Pb is a two-component mixture of common and radiogenic Pb, and that both the U–Pb and Pb–Pb isotope systems are concordant. In this circumstance, the analyses will lie — by amounts proportional to their common-Pb contents — along a mixing line between initial $^{207}Pb/^{206}Pb$ (calculated according to the model of Stacey and Kramers, 1975) and radiogenic Pb, on concordia. The analyses of all minerals of the same age will lie within uncertainty of a single regression line anchored at initial Pb; data falling significantly to the left of the mixing line suggest the presence of xenocrystic material, whereas dispersion to the right may indicate ancient or recent radiogenic-Pb loss. The mean date is determined from the lower intercept of the mixing line with the concordia curve.

In cases where the 204-correction is inaccurate (as above), and the data can be assumed to be essentially concordant, a similar initial-Pb regression approach may be applied. This procedure, the '207-method' of common-Pb correction, extrapolates each measured composition along an initial-Pb mixing line to the concordia curve to yield the radiogenic (207-corrected) $^{238}U/^{206}Pb^*$ date.

Fractionation of $^{207}Pb/^{206}Pb$ ratios during zircon or baddeleyite analysis is monitored and corrections can be made, if necessary, by reference to the OGC1 zircon standard or the PBR2 baddeleyite standard (Table 1). Uncertainties associated with this correction are added in quadrature to the uncertainties of $^{207}Pb^*/^{206}Pb^*$ ratios and dates.

Ratios of $^{238}U/^{206}Pb^*$ measured in baddeleyite by ion microprobe have been shown to vary significantly and systematically with the relative orientation of the baddeleyite crystal structure and the direction of the primary ion beam (Wingate and Compston, 2000). Reliable and precise dates can therefore only be determined from $^{207}Pb^*/^{206}Pb^*$ ratios, which are unaffected by this phenomenon (Wingate et al., 1998), although $^{238}U/^{206}Pb^*$ ratios can still be used in a semiquantitative manner for assessing the concordance of results. Common-Pb correction in baddeleyite employs either ^{204}Pb, as with zircon, or the '208-method', whereby the proportion of common ^{206}Pb in measured ^{206}Pb (referred to as f208) is determined from the difference between the measured $^{208}Pb/^{206}Pb$ ratio and the radiogenic ratio expected for the age and measured $^{232}Th/^{238}U$ of the mineral (Hinthorne et al., 1979; Compston et al., 1984; Wingate et al., 1998). The 208-method is generally only applicable to minerals (typically baddeleyite and some zircons) having low $^{232}Th/^{238}U$, and may be employed in cases where it provides higher precision and lower dispersion than correction using ^{204}Pb.

Table 1. Relevant values for U–Th–Pb standards used in SHRIMP and LA-ICP-MS analyses by GSWA

Standard	*Mineral*	*^{238}U (ppm)*	*^{232}Th (ppm)*	*$^{238}U/^{206}Pb^*$ age (Ma)*	*$^{207}Pb^*/^{206}Pb^*$ age (Ma)*	*Reference*
CZ3	zircon	551	30	561.5	–	Pidgeon et al., 1994; Nasdala et al., 2008
M257	zircon	840	227	561.3	–	Nasdala et al., 2008
Temora 2	zircon	–	–	416.8	–	Black et al., 2004
BR266	zircon	909	201	559	–	Stern, 2001
OGC1	zircon	–	–	–	3465.4	Stern et al., 2009
GJ1	zircon	230	15	601.7	607	Jackson et al., 2004; Kylander-Clark et al., 2013
91500.0	zircon	80	30	1062.4	1065.4	Wiedenbeck et al., 1995
Plešovice	zircon	–	–	337.1	–	Sláma et al., 2008
PBR2 (Phalaborwa)	baddeleyite	–	–	–	2059.6	Wingate and Compston, 2000; Heaman, 2009
India	monazite	2890	36946	509	–	PD Kinny and C Clark, pers. comm., 2010
GM3	monazite	6495	60000	486.5	470.2	A Kennedy, written comm., 2017
44069	monazite	3389	25626	424.9	–	Aleinikoff et al., 2006
Stern 8153	monazite	3791	55288	512	–	Horstwood et al., 2016
Trebilcock	monazite	6333	–	272	–	Tomascak et al., 1996
Thompsons Mine	monazite	–	–	–	1766	Richter et al., 2019
DD90-26A	monazite	–	–	–	2671.1	D Davis, written comm., 2019

Note: OGC1 is the zircon standard obtained by Curtin University from the same rock from which standard OG1 was described by Stern et al. (2009)

Ratios of $^{206}Pb^+/^{238}U^+$ in monazite are calibrated to the known $^{206}Pb/^{238}U$ of the monazite standard (Table 1) using a linear relationship between $^{206}Pb^+/UO_2^+$ and UO^+/UO_2^+ (Kinny, 1997). Monazite generates an unresolvable isobaric interference on $^{204}Pb^+$, which may be $(^{232}Th^{144}Nd^{16}O_2)^{++}$ (Ireland et al., 1999; Kirkland et al., 2009). This interference has been observed to correlate with thorium content (Kinny, 1997). Excess $^{204}Pb^+$ counts are corrected against the India monazite standard (Table 1) assuming $^{206}Pb/^{238}U$ – $^{207}Pb/^{235}U$ age-concordance of the standard at a known thorium concentration. Fractionation of the $^{207}Pb/^{206}Pb$ ratio is typically observed when the retardation lens system is at operating voltage during monazite analysis. Fractionation of $^{207}Pb/^{206}Pb$ ratios is monitored and corrections can be made, if necessary, by reference to the GM3 monazite standard. Uncertainties associated with this correction are added in quadrature to the uncertainties of $^{207}Pb^*/^{206}Pb^*$ ratios and dates.

Uncertainties assigned to all isotopic ratios and dates for individual analyses reflect contributions arising from counting statistics and common-Pb correction. Ratios and dates based on $^{238}U/^{206}Pb^*$ include an external 'spot-to-spot' uncertainty, related to the reproducibility of the standard $^{238}U/^{206}Pb^*$ measurements (for most sessions this is taken to be a minimum of 0.50% [1σ]). The internal uncertainty arising from calibration against the reference standard is also included in individual $^{238}U/^{206}Pb^*$ ratios and dates reported in data tables. In rare cases, significant secular drift of standard $^{238}U/^{206}Pb^*$ dates during an analytical session may be addressed by fitting a LOWESS curve (Cleveland, 1979), as implemented in the program Squid 2.50 (Ludwig, 2009). Details of both the external spot-to-spot and internal calibration uncertainties are reported in the Geochronology Record for each sample.

LA-ICP-MS analytical procedures

Sample preparation

Sample preparation procedures for separated minerals analysed by LA-ICP-MS are identical to those described above for SHRIMP analysis. In situ analyses of minerals by LASS and LA-ICP-MS methods are conducted on 25 x 48 mm polished thin sections.

Mineral imaging and target selection

Sample imaging and target selection procedures for separated minerals within epoxy discs analysed by LA-ICP-MS are identical to those described above for those analysed by SHRIMP. Monazite crystals for in situ analysis are identified in polished thin sections using the TIMA. Monazites are imaged in detail using high-contrast BSE methods with a Tescan VEGA-3 SEM, to reveal internal structure and compositional zoning. Monazite crystals are selected for analysis based on their size (>20 µm) and petrographic (textural) setting. Multiple analyses on individual crystals target different zones to test for potential age differences, whereas areas containing cracks and inclusions are avoided.

LA-ICP-MS U–Th–Pb and trace element zircon analysis

Separated zircons mounted in epoxy disks are ablated using a Resonetics RESOlution M-50A-LR sampling system, incorporating a 193 nm Compex 102 excimer laser.

Following two cleaning pulses and a 15–30 s period of background analysis, samples are ablated for 22–40 s at a 5 Hz repetition rate, using a 24–50 µm beam spot and laser energy of 1.5 – 2.0 J·cm^{-2}. The sample cell is flushed by ultrahigh-purity helium (350 mL·min^{-1}) and nitrogen (3.6 mL·min^{-1}). Intensities of the ion signals are measured using either an Agilent 7700s or 8900s quadrupole ICP-MS, with high-purity argon as the plasma gas.

For U–Th–Pb geochronology, mainly applied to detrital zircons, the isotopes measured typically include: ^{29}Si, ^{91}Zr, ^{204}Pb, ^{206}Pb, ^{207}Pb, ^{208}Pb, ^{232}Th and ^{238}U. The dwell time is 0.01 s for ^{29}Si and ^{91}Zr, 0.1 s for ^{204}Pb, ^{206}Pb, ^{207}Pb and ^{208}Pb, and 0.0125 s for ^{232}Th and ^{238}U. During sessions in which U–Th–Pb isotopes and trace elements are measured together in separated crystals, the isotopes measured include some or all of: ^{29}Si, ^{31}P, ^{43}Ca, ^{49}Ti, ^{51}V, ^{57}Fe, ^{63}Cu, ^{88}Sr, ^{89}Y, ^{91}Zr, ^{93}Nb, ^{95}Mo, ^{118}Sn, ^{139}La, ^{140}Ce, ^{141}Pr, ^{146}Nd, ^{147}Sm, ^{151}Eu, ^{157}Gd, ^{159}Tb, ^{163}Dy, ^{165}Ho, ^{166}Er, ^{169}Tm, ^{172}Yb, ^{175}Lu, ^{178}Hf, ^{181}Ta, ^{182}W, ^{204}Pb, ^{206}Pb, ^{207}Pb, ^{208}Pb, ^{232}Th and ^{238}U. In each scan of the mass spectrum, the dwell time for most isotopes is 0.01 s, with the exception of ^{88}Sr (0.02 s), ^{139}La (0.04 s), ^{141}Pr (0.04 s), ^{204}Pb, ^{206}Pb, ^{207}Pb and ^{208}Pb (each 0.03 s), ^{232}Th (0.0125 s), and ^{238}U (0.0125 s).

A block of standards is typically measured after every 15–20 unknown analyses, and includes zircon standards GJ-1, 91500, Plešovice and OGC1 (Table 1) as well as international glass standards NIST 610 and 612.

LA-ICP-MS U–Th–Pb monazite analysis

Monazite crystals in polished thin sections are ablated using a Resonetics RESOlution M-50A-LR sampling system, incorporating a Compex 102 excimer laser, or using a Teledyne Photon ANALYTE G2 UV Excimer Laser Ablation System. Following two cleaning pulses and a 40 s period of background analysis, samples are ablated for 15 s at a 4–7 Hz repetition rate, using a 7–20 µm beam diameter and laser energy of 1.5 – 2.0 J·cm^{-2}. The sample cell is flushed by ultrahigh-purity helium (320 mL·min^{-1}) and nitrogen (1.2 mL·min^{-1}). Intensities of the ion signals are measured using an Agilent 8900s quadrupole ICP-MS, Nu Plasma II MC-ICP-MS, or Thermo-Finnigan Element XR ICP-MS, with high-purity argon as the plasma gas.

For U–Th–Pb geochronology, the isotopes measured typically include: ^{238}U, ^{232}Th, ^{208}Pb, ^{207}Pb, ^{206}Pb, ^{204}Pb and ^{202}Hg over a 0.8 s integration time. A block of standards is analysed between every 10–20 unknown sample analyses, and typically includes monazite reference materials 44069, Stern 8153, Thompsons Mine, Trebilcock, India and DD90-26A (Table 1).

LASS U–Th–Pb and trace element monazite analysis

Monazite crystals in polished thin sections are ablated using a Resonetics RESOlution M-50A-LR sampling system, incorporating a Compex 102 excimer laser and equipped with a Laurin Technic S155 cell. Two cleaning pulses are followed by 40 s of background analysis, 20 s of sample analysis and another 15 s of background counting using a 7 µm beam diameter, repetition rate of 4 Hz and laser energy of 0.7 J·cm^{-2}. The sample cell is flushed with ultrahigh-purity helium (320 mL·min^{-1}) and nitrogen (1.2 mL·min^{-1}). Ablated products are split evenly between a Nu Plasma II MC-ICP-MS (for U–Th–Pb geochronology) and an Agilent 7700s or 8900 QQQ quadrupole ICP-MS (for trace elements), using high-purity Ar as the plasma gas.

On the MC-ICP-MS, ^{238}U, ^{232}Th, ^{208}Pb, ^{207}Pb, ^{206}Pb, ^{204}Pb and ^{202}Hg are monitored over a 0.8 s integration time. On the quadrupole ICP-MS, ^{28}Si, ^{31}P, ^{44}Ca, ^{88}Sr, ^{89}Y, ^{139}La, ^{140}Ce, ^{141}Pr, ^{146}Nd, ^{147}Sm, ^{151}Eu, ^{157}Gd, ^{159}Tb, ^{163}Dy, ^{165}Ho, ^{166}Er ^{169}Tm, ^{175}Lu, ^{178}Hf, ^{232}Th and ^{238}U are monitored for 0.01 or 0.02 s each.

A block of standards is analysed between every 10–20 unknown sample analyses, and typically includes monazite reference materials 44069, Stern 8153, Trebilcock, India and DD90-26A (Table 1), and a suite of well-characterized in-house monazite standards.

LA-ICP-MS zircon and monazite data reduction

Time-resolved mass spectra are reduced in Iolite 4 (Paton et al., 2011). Data reduction in Iolite include subtraction of baselines, internal standard calibration, correction for mass fractionation and instrument drift, and uncertainty propagation (Paton et al., 2011, and references therein). The time-resolved signals are used to identify and exclude contributions from inclusions of non-target minerals and to integrate the most stable and robust portion of each laser analysis.

The *U–Pb Geochronology* data reduction scheme in Iolite is used to reduce the U–Th–Pb isotope data (Paton et al., 2011). For zircon, the standard GJ-1 is generally used as the primary reference material, and 91500, OGC1 and Plešovice serve as secondary standards for quality control. For monazite, the standard 44069 is generally used as the primary reference material for age determination, with Stern 8163, Thompsons Mine, Trebilcock, India and DD90-26A (Table 1) as secondary standards for quality control. Accuracy is estimated as percent difference between measured age and true age of the secondary standard with <1% being considered acceptable. Typically, ^{238}U is chosen as the index channel and data for zircon and monazite are corrected for downhole elemental fractionation using the model in Iolite which best fits the data (Paton et al., 2010).

The uncertainty propagation protocols of Paton et al. (2010) are used to obtain the total uncertainty, in which the excess uncertainty for each analytical session required to account for all unquantified sources of analytical uncertainty is combined in quadrature with the internal precision of each individual analysis. The isotope ratios and their propagated uncertainties are exported from Iolite and then used to calculate dates in Isoplot 3.71 (Ludwig, 2003). Owing to the ubiquitous presence of ^{204}Hg in the argon carrier gas, which interferes with ^{204}Pb determinations in LA-ICP-MS analyses, a ^{204}Pb-based common Pb correction cannot be applied. As described above for SHRIMP analyses, the 208-correction can be employed for low-Th/U samples, and the 207-correction can be used to determine radiogenic

$^{238}U/^{206}Pb$ ratios for relatively young samples (<1000 Ma). Dates from analyses for which $^{238}U/^{206}Pb$ ratios indicate dates <1000 Ma are based on 207-corrected $^{238}U/^{206}Pb^*$ ratios; those >1000 Ma are based on uncorrected $^{207}Pb/^{206}Pb$ ratios.

The *Trace Elements* data reduction scheme in Iolite is used to reduce element concentration data for zircon (Paton et al., 2011). Glass standard NIST 610 is used as the primary reference material and NIST 612 as a secondary standard for quality control. The internal standard element is ^{29}Si, assumed to make up 14.76 wt% in zircon. Analytical accuracy is estimated as percent difference for multiple analyses of NIST 612 with values within 10% for most elements. Analytical precision, calculated as the coefficient of variation (s.d./mean), is <5% for most elements.

Trace element concentrations are filtered to systematically exclude analyses contaminated by inclusions too small to detect in the time-resolved signal (Lu et al., 2016, 2019). La >1 ppm is taken to reflect apatite contamination, which is the most commonly recognized contaminant in zircon, Fe >5000 ppm is taken to indicate contamination by Fe oxide minerals, and Ti >50 ppm is taken to indicate contamination by Ti-(Fe-)oxide minerals.

The *Trace Elements* data reduction scheme in Iolite is also used to reduce the element concentration data for monazite (Paton et al., 2011). A series of well-characterized in-house monazite standards with known Ce contents are used to plot an external calibration curve, from which the Ce content of each unknown is determined. To determine trace element contents, VK-1 is used as the primary trace element standard with ^{140}Ce as the internal reference for Si, P, Ca, Y, La, Pr, Nd, Sm, Eu, Gd, Tb, Dy, Er, Tm, Lu, Hf, Th and U, and 44069 is the primary standard for Tb, Ho, Tm and Sr (Table 1). In-house monazite reference materials and 44069 are monitored as secondary standards for quality control. Analytical accuracy is estimated as percent difference for multiple analyses of the secondary standards with values better than 10% for most elements and <20% for heavy REE owing to their low concentrations.

Data interpretation

Weighted mean dates are determined for groups of analyses by weighting each $^{207}Pb/^{206}Pb$ or $^{238}U/^{206}Pb$ date by the inverse of its variance (the square of its $1\sigma_i$ analytical uncertainty). Dispersion of results beyond their individual analytical uncertainties ($2.5\sigma_i$) suggests the presence of geological sources of uncertainty, such as the inclusion of analyses of slightly older xenocrysts, or the inclusion of analyses that reflect loss of radiogenic Pb.

In the case of dispersed data, dates lying farthest from the weighted mean value are excluded progressively from the group until all remaining analyses are within $\pm2.5\sigma_i$ of the weighted mean value. For igneous samples analyses beyond $\pm2.5\sigma_i$ can typically be attributed to Group X or P (Table 2), and for detrital samples they are not included in the maximum depositional age and remain in Group S. For some samples, it may not be possible to confidently attribute dispersion to either the presence of xenocrystic material or to minor loss of radiogenic Pb, and it may be reasonable to retain dates that differ from the weighted mean by amounts in excess of the $2.5\sigma_i$ limits. Weighted mean dates are reported with 95% confidence intervals, defined as the 1σ internal uncertainty of the weighted mean $^{207}Pb^*/^{206}Pb^*$ (or $^{238}U/^{206}Pb^*$) ratio or date, multiplied by the square root of the MSWD and by Students t for $n-1$ degrees of freedom. Uncertainties of weighted mean $^{238}U/^{206}Pb^*$ dates determined by SHRIMP also include reproducibility and calibration uncertainties.

In cases where the true location of the mean data point can be assumed to fall on the concordia curve, it is possible to calculate a 'concordia age' (Ludwig, 1998), which makes use of both $^{207}Pb^*/^{206}Pb^*$ and $^{238}U/^{206}Pb^*$ ratios. This approach will typically yield a more precise mean age than can be obtained using either ratio alone, and also yields an objective and quantitative measure of concordance.

Data presentation

Both the $^{238}U/^{206}Pb$ and $^{207}Pb/^{206}Pb$ ratios (not corrected for common Pb), and the $^{238}U/^{206}Pb^*$ and $^{207}Pb^*/^{206}Pb^*$ ratios (common-Pb corrected), are listed in data tables for SHRIMP, whereas only uncorrected ratios are listed for LA-ICP-MS. Individual analyses in data tables are placed into interpretative groups (Table 2). Uncertainties in data tables and error bars in figures are at the 1σ level. Listed sample numbers are GSWA sample numbers, unless stated otherwise. Within the text, capitalized names refer to standard 1:250 000 and 1:100 000 map sheets; where 1:100 000 and 1:250 000 map sheets have the same name, the 1:100 000 sheet is implied unless otherwise indicated.

U–Pb data are presented using 'inverse' or 'Tera–Wasserburg' concordia diagrams (Tera and Wasserburg, 1972). These diagrams have several advantages over 'conventional' concordia diagrams (Wetherill, 1956) for ion microprobe and LA-ICP-MS analyses. The two main age-sensitive ratios measured using the SHRIMP ($^{207}Pb^*/^{206}Pb^*$ and $^{238}U/^{206}Pb^*$), and LA-ICP-MS ($^{207}Pb/^{206}Pb$ and $^{238}U/^{206}Pb$), are plotted directly on Tera–Wasserburg diagrams, whereas conventional diagrams use $^{206}Pb^*/^{238}U$ and $^{207}Pb^*/^{235}U$. However, ^{235}U is not directly measured using SHRIMP or LA-ICP-MS, and conventional diagrams do not show $^{207}Pb^*/^{206}Pb^*$ ratios, which are the most sensitive indicator of age for minerals >1000 Ma. In addition, Tera–Wasserburg diagrams avoid the strong correlation of uncertainties that visually 'skews' data on a conventional diagram. Tera–Wasserburg diagrams also facilitate the processing of data without explicit correction for common Pb, which is useful in cases where the ^{204}Pb-based common-Pb correction is inaccurate.

Table 2. Group IDs used in interpretation of U–Pb analyses

Group ID	*Interpretation*	*Group ID*	*Interpretation*
I	magmatic	Y	youngest detrital grain
X	xenocrystic	S	older detrital grains
P	radiogenic-Pb loss	D	excluded analyses
M	metamorphic	M2	second metamorphic event
M3	third metamorphic event	Z	defined individually

In addition to presentation on concordia diagrams, dates obtained for zircons from sedimentary rock samples are displayed on combined probability density and histogram diagrams. These are used to illustrate the distribution of detrital zircon dates (age spectrum). These diagrams present two cumulative probability density curves: one includes all analyses, and the other includes only accepted data (typically those less than 5 or 10% discordant, and with <1% common ^{206}Pb). The height and width of each age peak is proportional to the number and precision of data points making up the peak. The integrated histogram indicates the approximate number of analyses in each peak. Dates for Mesoproterozoic and older detrital zircons are generally based on ^{207}Pb*/^{206}Pb* ratios, whereas those for younger minerals are based on ^{238}U/^{206}Pb* ratios. The precise age at which the change is made from one ratio to the other is generally between about 800 and 1000 Ma, and is determined from the age characteristics for each sample.

Abbreviations and formulae used in Geochronology Records

Pb* = radiogenic Pb

f204 (%) = 100 × (common ^{206}Pb/total ^{206}Pb), assessed using measured ^{204}Pb/^{206}Pb

f207 (%) = 100 × (common ^{206}Pb/total ^{206}Pb), assessed using measured ^{207}Pb/^{206}Pb and assuming concordance

f208 (%) = 100 × (common ^{206}Pb/total ^{206}Pb), assessed using measured ^{208}Pb/^{206}Pb, ^{232}Th/^{238}U, and date

Discordance (%) = 100 × [(^{207}Pb/^{206}Pb date)–(^{238}U/^{206}Pb date)]/(^{207}Pb/^{206}Pb date)

References

Aleinikoff, JN, Schenck, WS, Plank, MO, Srogi, L, Fanning, CM, Kamo, SL and Bosbyshell, H 2006, Deciphering igneous and metamorphic events in high-grade rocks of the Wilmington Complex, Delaware: Morphology, cathodoluminescence and backscattered electron zoning and SHRIMP U–Pb geochronology of zircon and monazite: GSA Bulletin, v. 118, p. 39–64.

Bastian, LV 1994, The dune systems of the Swan coastal plain: subdivision based on mineral trends in the surface soils: Chemistry Centre of Western Australia, Report of Investigation 41, 45p.

Black, LP, Kamo, SL, Allen, CM, Davis, DW, Aleinikoff, JN, Valley, JW, Mundil, R, Campbell, IH, Korsch, RJ, Williams, IS and Foudoulis, C 2004, Improved ^{206}Pb/^{238}U microprobe geochronology by the monitoring of a trace element related matrix effect: SHRIMP, ID-TIMS, ELA-ICP-MS, and oxygen isotope documentation for a series of zircon standards: Chemical Geology, v. 205, p. 115–140.

Claoué-Long, JC, Compston, W, Roberts, J and Fanning, CM 1995, Two Carboniferous ages: a comparison of SHRIMP zircon dating with conventional zircon ages and ^{40}Ar/^{39}Ar analysis, *in* Time Scales and Global Stratigraphic Correlation *edited by* WA Berggren, DV Kent, M-P Aubrey and J Hardenbol: Society for Sedimentary Geology, Special Publication 54, p. 3–21.

Cleveland, WS 1979, Robust, locally weighted regression and smoothing scatterplots: Journal of the American Statistical Association, v. 74, p. 829–836.

Compston, W, Williams, IS and Meyer, C 1984, U–Pb geochronology of zircons from lunar breccia 73217 using a sensitive high mass-resolution ion microprobe: Journal of Geophysical Research, v. 89, p. B252–B534.

Heaman, LM 2009, The application of U–Pb geochronology to mafic, ultramafic and alkaline rocks: an evaluation of three mineral standards: Chemical Geology, v. 261, p. 43–52.

Hinthorne, JR, Andersen, CA, Conrad, RL and Lovering, JF 1979, Single-grain ^{207}Pb/^{206}Pb and U/Pb age determinations with a 10 µm spatial resolution using the ion microprobe mass analyzer (IMMA): Chemical Geology, v. 25, p. 271–303.

Horstwood, MSA, Kosler, J, Gehrels, G, Jackson, SE, McLean, NM, Paton, C, Pearson, NJ, Sircombe, K, Sylvester, P, Vermeesch, P, Bowring, JF, Condon, DJ and Schoene, B 2016, Community-derived standards for LA-ICP-MS U–(Th-)Pb geochronology – Uncertainty propagation, age interpretation and data reporting: Geostandards and Geoanalytical Research, v. 40, p. 311–332.

Ireland, TR, Wooden, JL, Persing, H and Ito, B 1999, Geological applications and analytical development of the SHRIMP-RG: EOS Transactions, American Geophysical Union 80, article no. F1117.

Jackson, SE, Pearson, NJ, Griffin, WL, and Belousova, EA 2004, The application of laser ablation-inductively coupled plasma-mass spectrometry to in situ U/Pb zircon geochronology: Chemical Geology, v. 211, p. 47–69.

Kinny, PD 1997, Users' guide to U–Th–Pb dating of titanite, perovskite, monazite, and baddeleyite using the WA SHRIMP: Curtin University of Technology, School of Physical Sciences, Report SPS693/1997/AP72, 21p.

Kirkland, CL, Whitehouse, MJ and Slagstad, T 2009, Fluid-assisted zircon and monazite growth within a shear zone; a case study from Finnmark, Arctic Norway: Contributions to Mineralogy and Petrology, v. 158, p. 637–657.

Kylander-Clark, ARC, Hacker, BR and Cottle, JM 2013, Laser-ablation split-stream ICP petrochronology: Chemical Geology, v. 345, p. 99–112.

Lu, Y, Loucks, RR, Fiorentini, ML, McCuaig, TC, Evans, NJ, Yang, Z-M, Hou, Z-Q, Kirkland, CL, Parra-Avila, LA and Kobussen, A 2016, Zircon compositions as a pathfinder for porphyry Cu ± Mo ± Au deposits: Society of Economic Geologists Special Publication 19, p. 329–347.

Lu, Y, Smithies, RH, Wingate, MTD, Evans, NJ, McCuaig, TC, Champion, DC and Outhwaite, M 2019, Zircon fingerprinting of magmatic–hydrothermal systems in the Archean Yilgarn Craton: Geological Survey of Western Australia, Report 197, 22p.

Ludwig, KR 1998, On the treatment of concordant uranium–lead ages: Geochimica et Cosmochimica Acta, v. 62, p. 665–676.

Ludwig, KR 2003, Isoplot 3.00; A geochronological toolkit for Microsoft Excel: Berkeley Geochronology Centre, Special Publication 4, 70p.

Ludwig, KR 2009, Squid 2.50, A User's Manual: Berkeley Geochronology Centre, Berkeley, California, USA, 95p. (unpublished report).

Nasdala, L, Hofmeister, W, Norberg, N, Mattinson, JM, Corfu, F, Dörr, W, Kamo, SL, Kennedy, AK, Kronz, A, Reiners, PW, Frei, D, Kosler, J, Wan, Y, Götze, J, Häger, T, Kröner, A and Valley, JW 2008, Zircon M257 — a homogeneous natural reference material for the ion microprobe U–Pb analysis of zircon: Geostandards and Geoanalytical Research, v. 32, p. 247–265.

Paton, C, Woodhead, JD, Hellstrom, JC, Hergt, JM, Greig, A and Maas, R 2010, Improved laser ablation U-Pb zircon geochronology through robust downhole fractionation correction: Geochemistry, Geophysics, Geosystems, v. 11, 36p., doi:10.1029/2009GC002618.

Paton, C, Hellstrom, J, Paul, B, Woodhead, J and Hergt, J 2011, Iolite: freeware for the visualization and processing of mass spectrometer data: Journal of Analytical Atomic Spectrometry, v. 26, p. 2508–2518.

Pidgeon, RT, Furfaro, D, Kennedy, AK, Nemchin, AA and Van Bronswijk, W 1994, Calibration of zircon standards for the Curtin SHRIMP II, *in* Eighth International Conference on Geochronology, Cosmochronology, and Isotope Geology — Abstracts: United States Geological Survey, Circular 1107, p. 251.

Richter, M, Nebel-Jacobsen, Y, Nebel, Y, Zack, T, Mertz-Kraus, R, Raveggi, M and Rösel, D 2019, Assessment of five monazite reference materials for U–Th/Pb dating using laser-ablation ICP-MS: Geosciences, v. 9, p. 391.

Sláma, J, Košler, J, Condon, DJ, Crowley, JL, Gerdes, A, Hanchar, JM, Horstwood, MSA, Morris, GA, Nasdala, L, Norberg, N, Schaltegger, U, Schoene, B, Tubrett, MN and Whitehouse, MJ 2008, Plešovice zircon — a new natural reference material for U–Pb and Hf isotopic microanalysis: Chemical Geology, v. 249, p. 1–35.

Stacey, JS and Kramers, JD 1975, Approximation of terrestrial lead isotope evolution by a two-stage model: Earth and Planetary Science Letters, v. 26, p. 207–221.

Steiger, RH and Jäger, E 1977, Subcommission on geochronology: convention on the use of decay constants in geo- and cosmochronology: Earth and Planetary Science Letters, v. 36, p. 359–362.

Stern, RA 2001, A new isotopic and trace-element standard for the ion microprobe: preliminary thermal ionization mass spectrometry (TIMS) U–Pb and electron-microprobe data: Geological Survey of Canada, Radiogenic Age and Isotopic Studies, Report 14, Current Research 2001-F1, 11p.

Stern, RA, Bodorkos, S, Kamo, SL, Hickman, AH and Corfu, F 2009, Measurement of SIMS instrumental mass fractionation of Pb isotopes during zircon dating: Geostandards and Geoanalytical Research, v. 33, p. 145–168.

Tera, F and Wasserburg, GJ 1972, U–Th–Pb systematics in three Apollo 14 basalts and the problem of initial Pb in lunar rocks: Earth and Planetary Science letters, v. 14, p. 281–304.

Tomascak, PB, Krogstad, EJ and Walker, RJ 1996, U-Pb monazite geochronology of granitic rocks from Maine: Implications for Late Paleozoic tectonics in the Northern Appalachians: The Journal of Geology, v. 104, p. 185–195.

Wetherill, GW 1956, Discordant uranium–lead ages: Transactions of the American Geophysical Union, v. 37, p. 320–326.

Wiedenbeck, M, Allé, P, Corfu, F, Griffin, WL, Meier, M, Oberli, F, von Quadt, A, Roddick, JC and Spiegel, W 1995, Three natural zircon standards for U–Th–Pb, Lu-Hf, trace element and REE analyses: Geostandards Newsletter, v. 19, p. 1–23.

Williams, IS 1998, U–Th–Pb geochronology by ion microprobe, *in* Applications of microanalytical techniques to understanding mineralizing processes *edited by* MA McKibben, WC Shanks III and WI Ridley: Reviews in Economic Geology, v. 7, p. 1–35.

Williams, IS, Buick, IS and Cartwright, I 1996, An extended episode of early Mesoproterozoic metamorphic fluid flow in the Reynolds Range, central Australia: Journal of Metamorphic Geology, v. 14, p. 29–47.

Wingate, MTD and Compston, W 2000, Crystal orientation effects during ion microprobe U–Pb analysis of baddeleyite: Chemical Geology, v. 168, p. 75–97.

Wingate, MTD, Campbell, IH, Compston, W and Gibson, GM 1998, Ion microprobe U–Pb ages for Neoproterozoic basaltic magmatism in south-central Australia and implications for the breakup of Rodinia: Precambrian Research, v. 87, p. 135–159.

RECORD 2024/1

INTRODUCTION TO GEOCHRONOLOGY INFORMATION, 2024

IOH Fielding, RE Turnbull and Y Lu

Access GSWA products

All products
All GSWA products are free to download as PDFs from the DEMIRS eBookshop <www.demirs.wa.gov.au/ebookshop>.
View other geoscience information on our website <www.demirs.wa.gov.au/gswa>.

Hard copies
Limited products are available to purchase as hard copies from the First Floor Counter at Mineral House or via the DEMIRS eBookshop <www.demirs.wa.gov.au/ebookshop>.

Fieldnotes
Fieldnotes is a free digital-only quarterly newsletter which provides regular updates to the State's exploration industry and geoscientists about GSWA's latest programs, products and services.
Access by subscribing to the GSWA eNewsletter <www.demirs.wa.gov.au/gswaenewsletter> or downloading the free PDF from the DEMIRS eBookshop <www.demirs.wa.gov.au/ebookshop>.

GSWA eNewsletter
The GSWA eNewsletter is an online newsletter that contains information on workshops, field trips, training and other events.
To keep informed, please subscribe <www.demirs.wa.gov.au/gswaenewsletter>.

Further details of geoscience products are available from:

First Floor Counter
Department of Energy, Mines, Industry Regulation and Safety
100 Plain Street
EAST PERTH WESTERN AUSTRALIA 6004
Phone: +61 8 9222 3459 Email: publications@dmirs.wa.gov.au
www.demirs.wa.gov.au/GSWApublications